

Plasmonic affinity biosensors: advances, challenges and applications

J. Homola

**Institute of Photonics and Electronics, Czech Academy of Sciences
Prague, Czech Republic**

Prague, March 3, 2026

History of plasmonic (bio)sensing

A brief history of surface plasmons and their use in optical sensing

1902: Wood observed anomalies in the spectrum of light diffracted on a metallic diffraction grating.

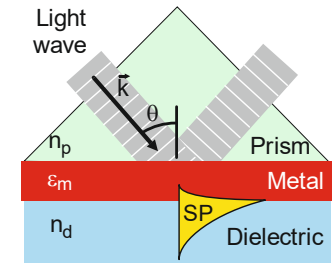
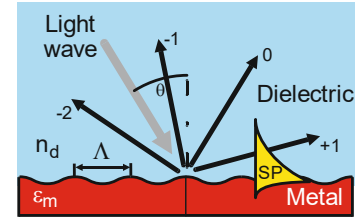
1941: Fano attributed these anomalies to surface electromagnetic waves.

1968: Otto, Kretschmann, and Raether developed a convenient method for the excitation of surface plasmons and ushered them into modern optics.

1982: Nylander and Liedberg reported the first use of surface plasmons for optical sensing.

Since then >10k research papers on optical biosensors have been published.

J. Homola, *Chemical Reviews*, 108, 462-493 (2008).



A brief history of surface plasmons and their use in optical sensing

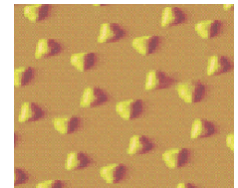
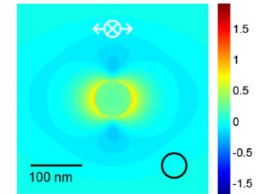
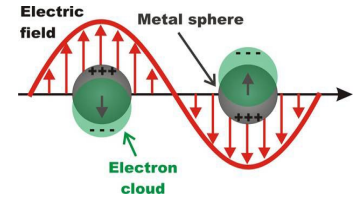
1997: Mirkin et al. used the localized surface plasmons on metallic nanoparticles in an aggregation-based assay.

1998: Englebienne reported the first biosensor based on localized surface plasmons on functionalized metallic nanoparticles in solution.

2002: Haes and Van Duyne reported a biosensors based on localized surface plasmons on metallic nanotriangles fabricated on a planar substrate.

Based on the first chip-based biosensor reports, biosensors based on plasmonic nanostructures are ~20 years younger.

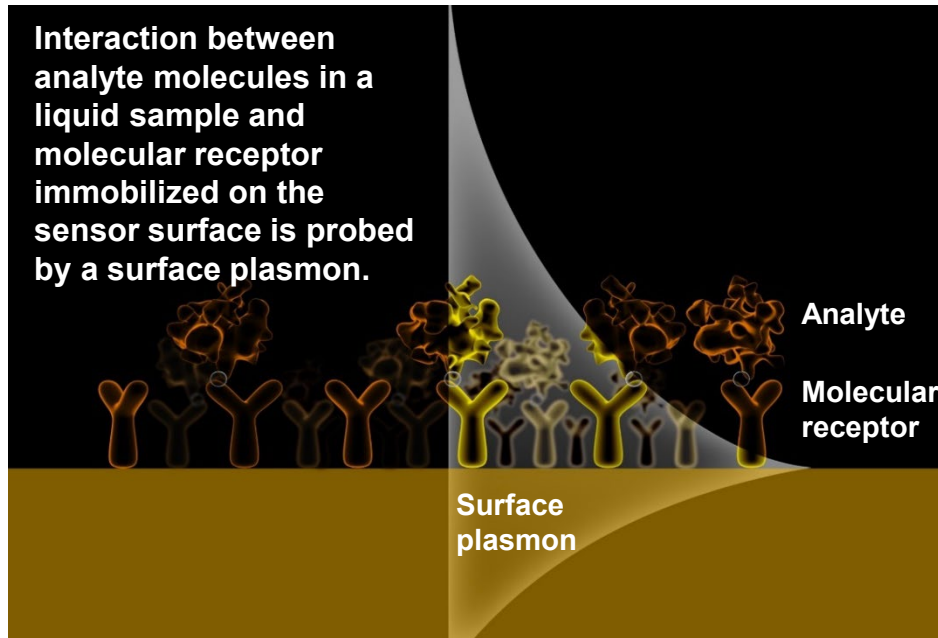
B. Špačková, P. Wrobel, M. Bocková, J. Homola, *Proc. IEEE*, 104, 2380–2408 (2016).
H. Altug, S.H. Oh, S.A. Maier, J. Homola, *Nature Nanotechnology*, 17, 5–16 (2022).



Introduction to plasmonic biosensing

Affinity biosensors based on surface plasmons

Plasmonic affinity biosensors: optical biosensors that employ special electromagnetic modes – surface plasmons – to probe the biomolecular interactions taking place at the sensor surface.



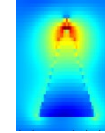
Main features:

- Direct.
- Real-time
- Label-free
- Sensitive.
- Non-invasive.

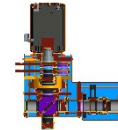
Plasmonic affinity biosensors: main components



**Plasmonic
(nano)structures**



**Optical sensing
platforms**



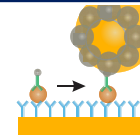
**Microfluidic
systems**



**Functional
coatings**



**Assays and
methodologies**

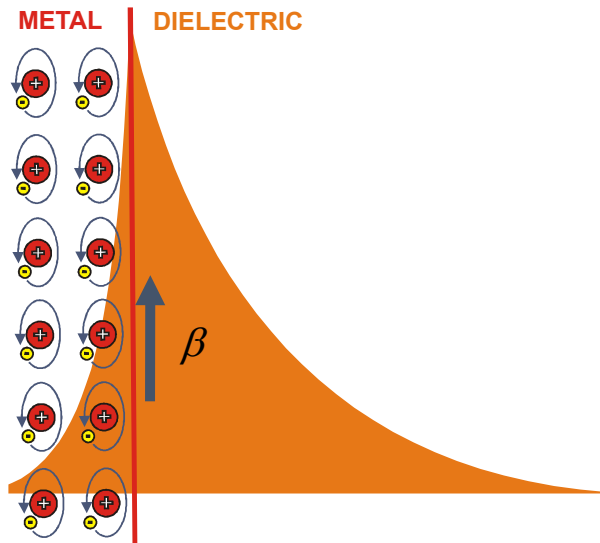


Plasmonic nanostructures

Surface plasmons

Surface plasmons (SPs) are entities of electromagnetic field that may exist at the interface between a metal and a dielectric.

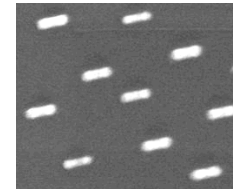
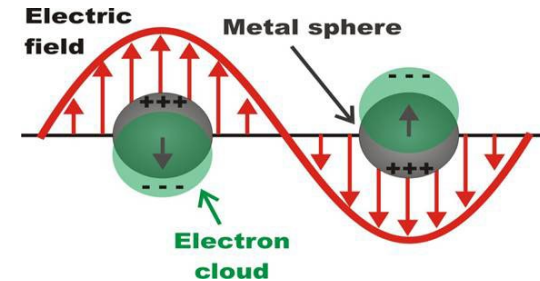
A. Propagating SPs



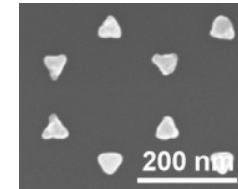
Field extent: $L_{\text{diel}} = 150 - 400 \text{ nm}$

J. Homola, *Chemical Reviews*, 108, 462-493 (2008).

B. Localized SPs



Gold nanorods.



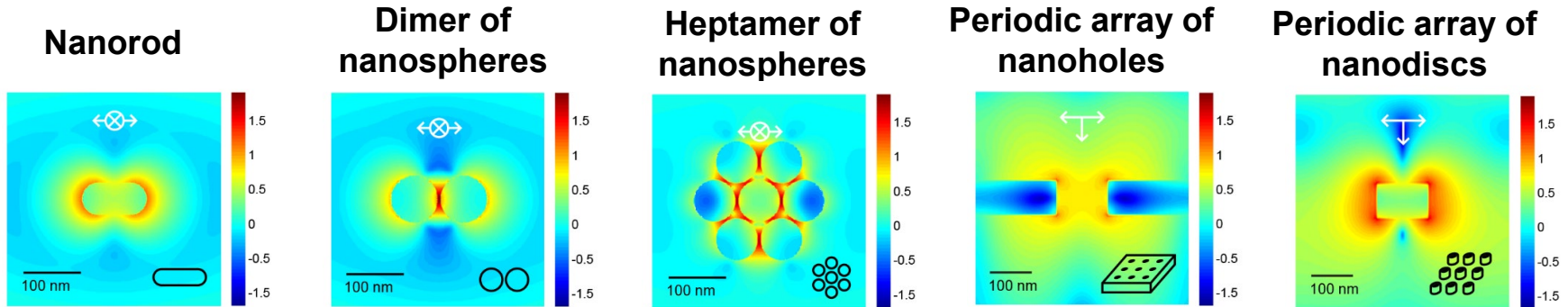
Nanopyramid array.

Field extent: $L_{\text{diel}} = 10 - 40 \text{ nm}$

B. Špačková, et al., *Proc. IEEE*, 104, 2380-2408 (2016).

Plasmonic nanostructures and affinity biosensing

The advancements in nanofabrication and computational techniques have stimulated the development of sophisticated nanophotonic structures and their sensing applications.



Electric field distribution in the vicinity of metal nanoobjects and their arrays.

- High confinement.
- Control of field distribution.
- Control of analyte transport.
- Cost-effective chip manufacturing.
- Spatially resolved functionalization.
- Integration and miniaturization.

H. Altug, S.H. Oh, S.A. Maier, J. Homola, *Nature Nanotechnology*, 17, 5–16 (2022).

Evaluating potential of plasmonic nanostructures for biosensing

Which plasmonic nanostructure is best for optical affinity biosensing?

Simple answer:

Figure of merit (FOM)

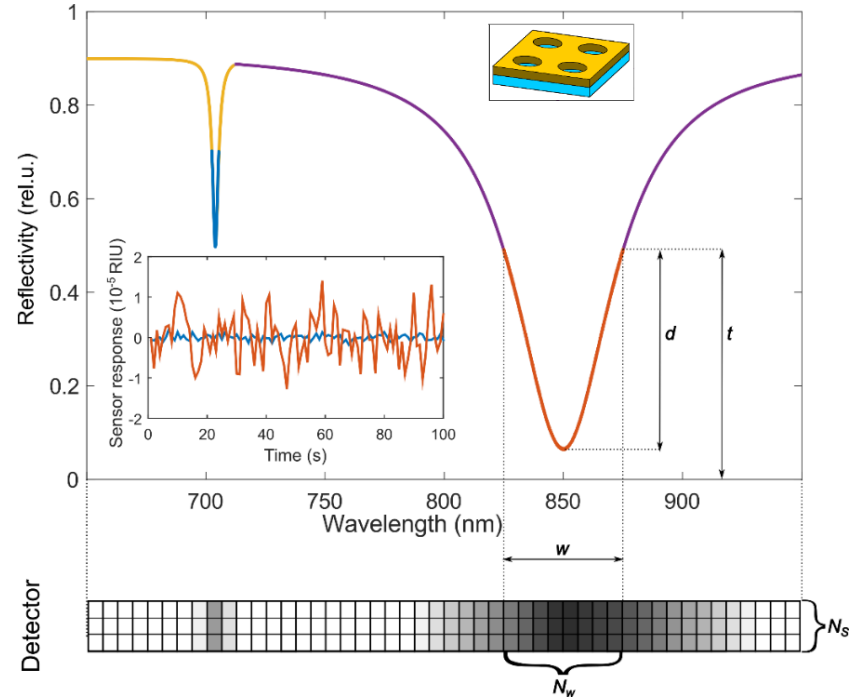
$$FOM = \frac{S}{w}$$

S ... sensitivity

w ... width of plasmonic feature

Correct answer:

It is more complicated!



Spectral reflectivity of nanohole array; the inset shows the sensor response-time series for the two resonances.

Evaluating potential of plasmonic nanostructures for biosensing

Analytical model for plasmonic sensor refractive index resolution (σ_{RI})

$$\sigma_{RI} = \left(\frac{1}{2\sqrt{N_T \cdot N_s \cdot N_w \cdot C}} \right) \left(\frac{\sqrt{t - 0.3d}}{d} \frac{1}{FOM} \right) = A \frac{1}{FOM^+}$$

N_T ... number of timely averaged intensities

N_s ... number of spatially averaged intensities

N_w ... number of points across the resonance

C ... capacity of photodetector (well depth)

t ... threshold of the centroid method

d ... depth of feature

Parameter A depends solely on the characteristics of the optoelectronic system.

New figure of merit FOM^+ is associated with the sensing structure and the coupling optics, which determine the characteristics of the resonance feature.

J. Slabý, J. Homola, *Biosensors & Bioelectronics*, 212, 114426 (2022).

Optical readout systems

Optical platforms: spectroscopy of surface plasmons

Main features:

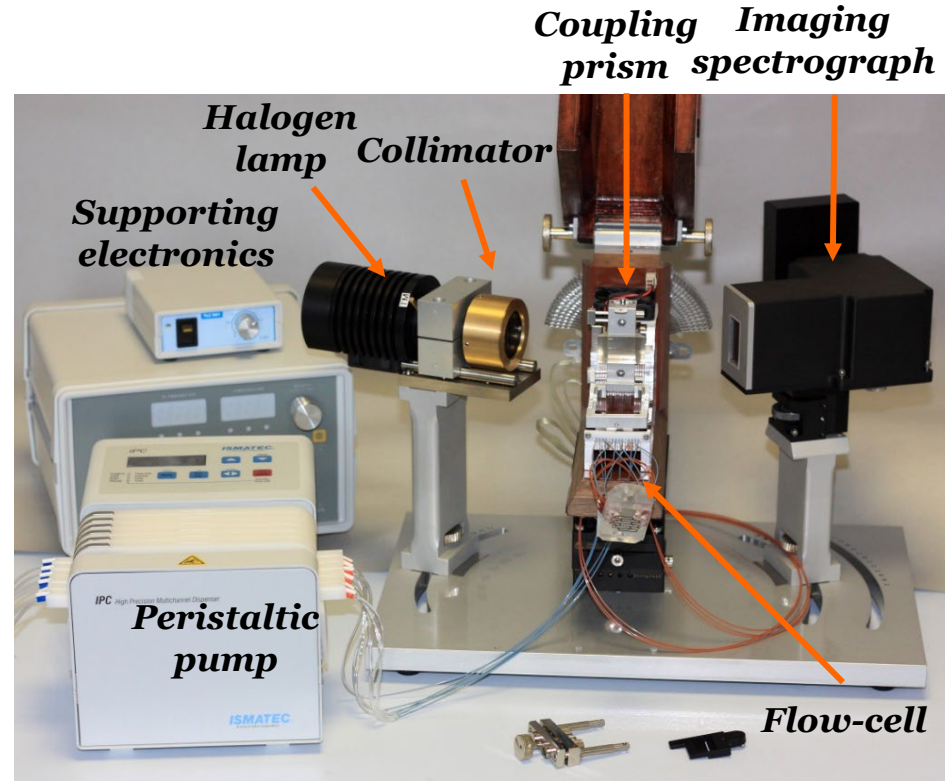
- Excitation of surface plasmons via the attenuated total reflection.
- Spectroscopy of surface plasmons on continuous or nanostructured metals.
- Temperature stabilization (stability $< 0.01^{\circ}\text{C}$).

RI resolution:

$< 5 \times 10^{-8}$ RIU

Number of channels:

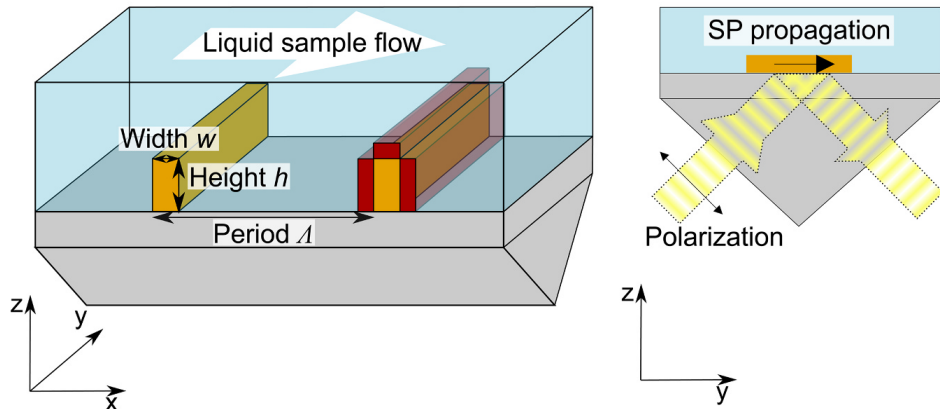
6



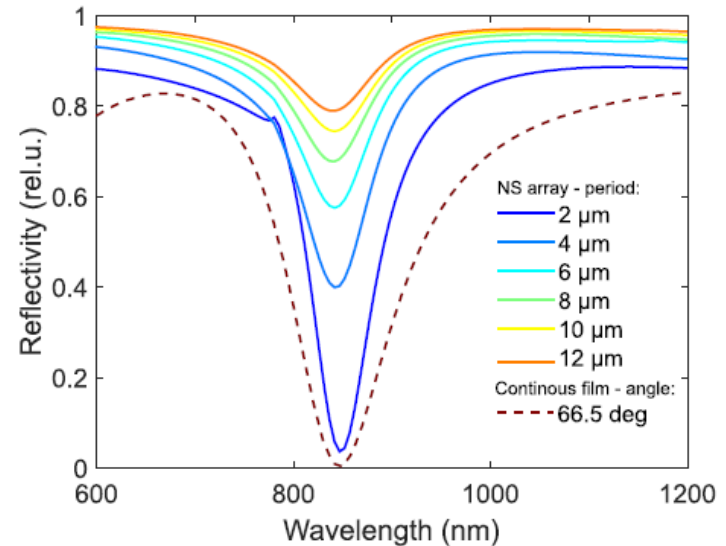
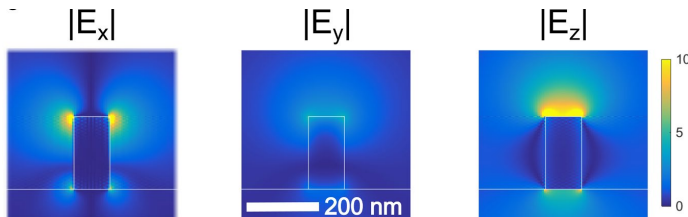
Optical platform for spectroscopy of surface plasmons based on the attenuated total reflection (ATR) and prism coupling.

Optical platform for spectroscopy of surface plasmons

Excitation of surface plasmons on an array of gold nanostripes.



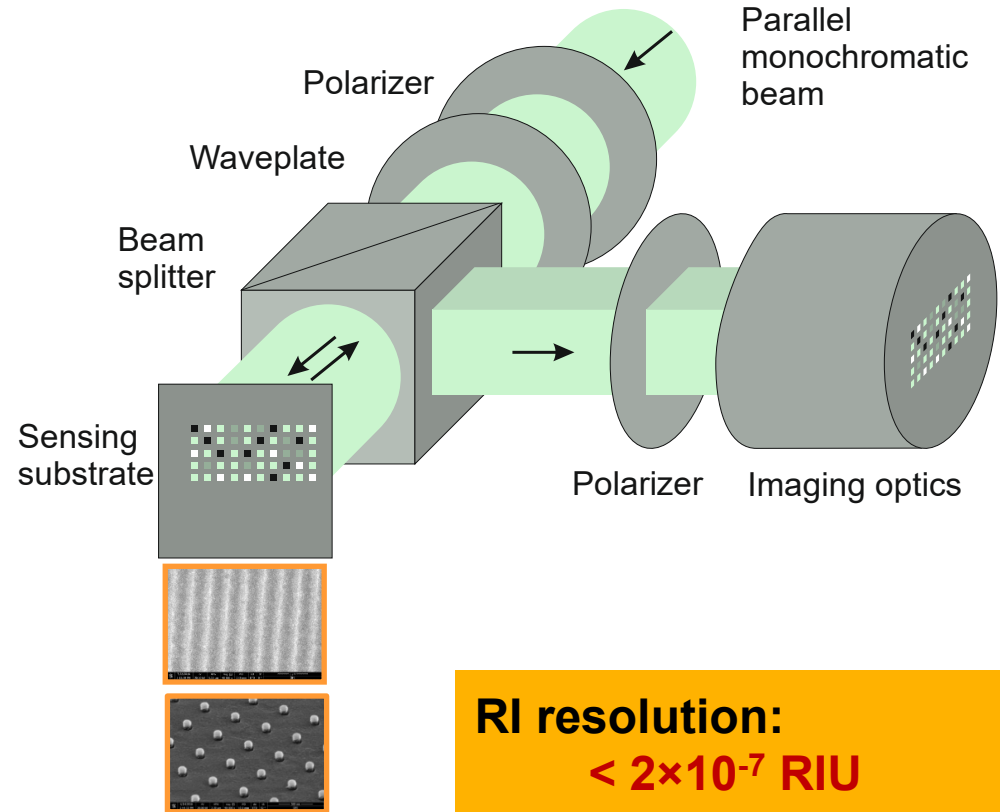
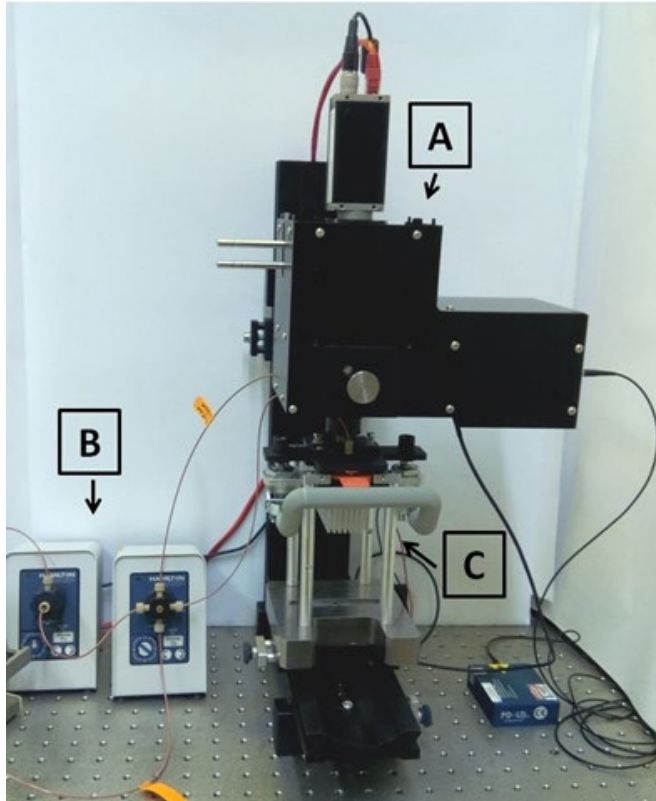
Scheme of gold nanostripe array and the excitation geometry (above); distribution of the electric field of plasmonic mode (below).



Reflectivity as a function of wavelength calculated for the different array periods.

J. Slabý, M. Bocková, J. Homola, *Sensors and Actuators B*, 130629 (2021).

Optical platforms: surface plasmon imaging



Laboratory prototype of an imaging platform based on diffractive coupling of light to surface plasmons (left) and schematic of the platform (right).

RI resolution:
 $< 2 \times 10^{-7}$ RIU

Number of channels:
50 – 70

Optical platforms: surface plasmon imaging based on gratings with a variable period

Excitation of surface plasmons on a diffraction grating.

Coupling condition:

$$\frac{2\pi}{\lambda} n \sin \alpha + m \frac{2\pi}{\Lambda} = \pm \operatorname{Re} \{ \beta \}$$

λ ... wavelength of the incident light

n ... refractive index of the dielectric

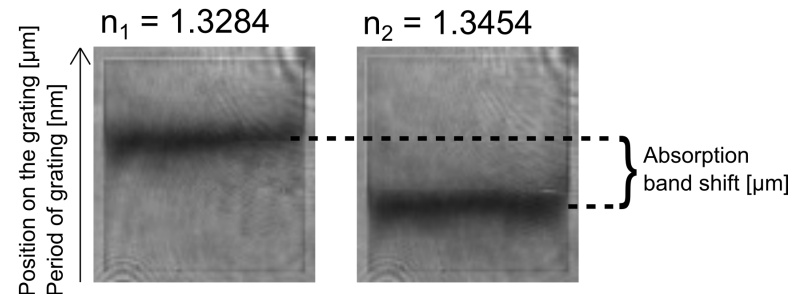
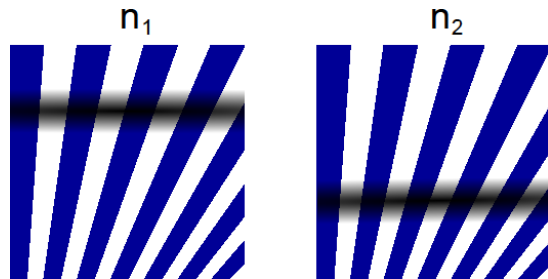
α ... angle of incidence

m ... order of diffraction

Λ ... period of the grating

β ... propagation constant of surface plasmon

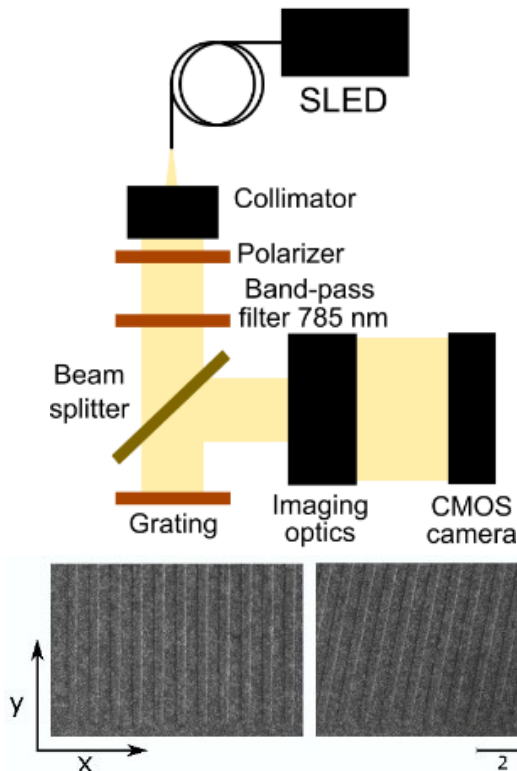
Principle of operation:



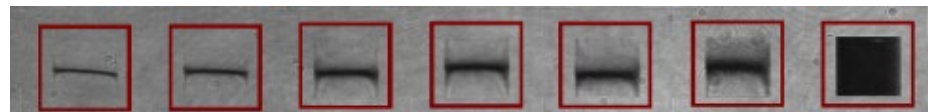
Excitation of surface plasmons on a diffraction grating with a linearly increasing period. Concept (left) and experimental demonstration (right).

J. Slabý et al., *Sensors and Actuators B: Chemical*, 453, 139502 (2026).

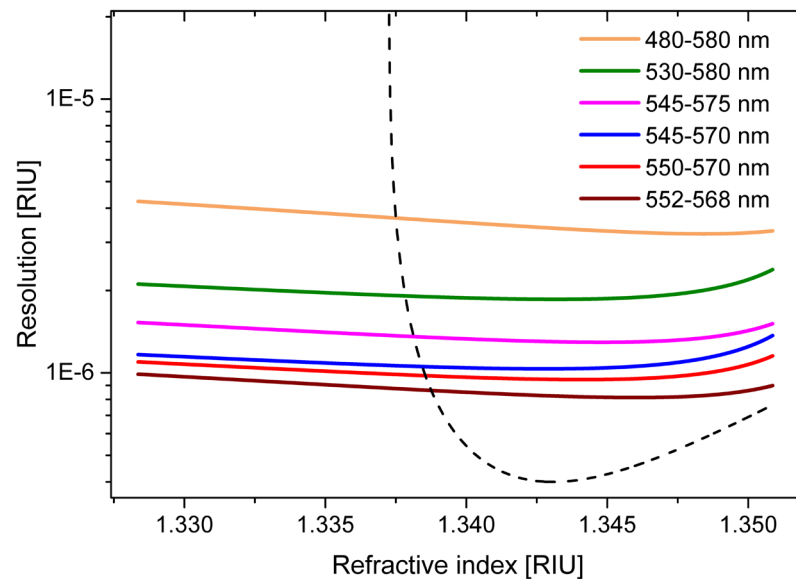
Optical platforms: surface plasmon imaging based on gratings with a variable period



Scheme of optical setup (top) and SEM image of conventional and variable period grating (bottom).



SPR images of six gratings with a variable period and one grating with a constant period.



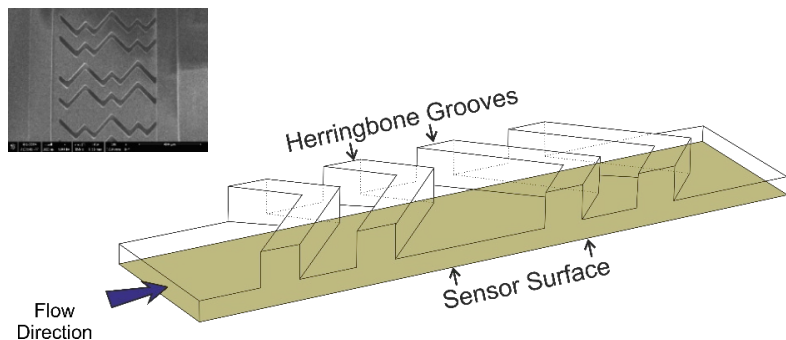
Refractive index resolution for gratings of different designs and grating with a constant period.

Microfluidic systems and analyte transport

Analyte transport in plasmonic biosensors

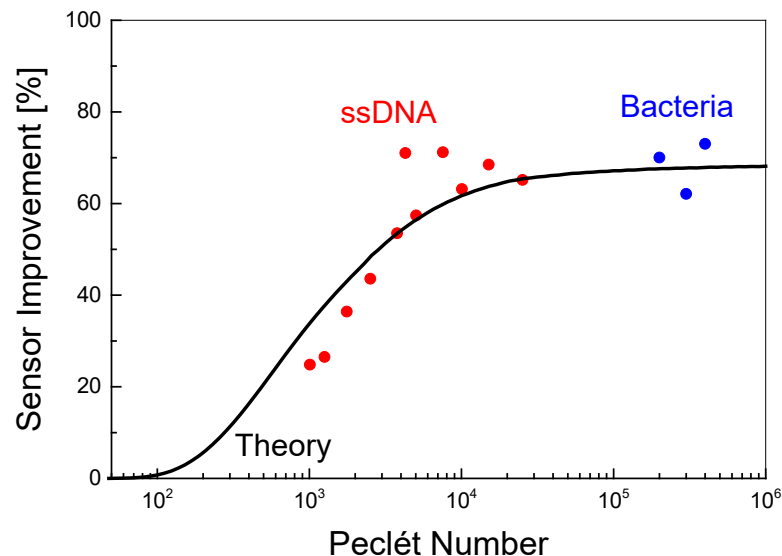
In plasmonic affinity biosensors, the interaction between analyte (in liquid sample) and receptors (on sensing surface) takes place in a flow cell.

The transport of analyte to an active surface of the sensor can be improved by passive mixing structures.



Scheme and a micrograph (top) of a herringbone micromixer in a microfluidic channel.

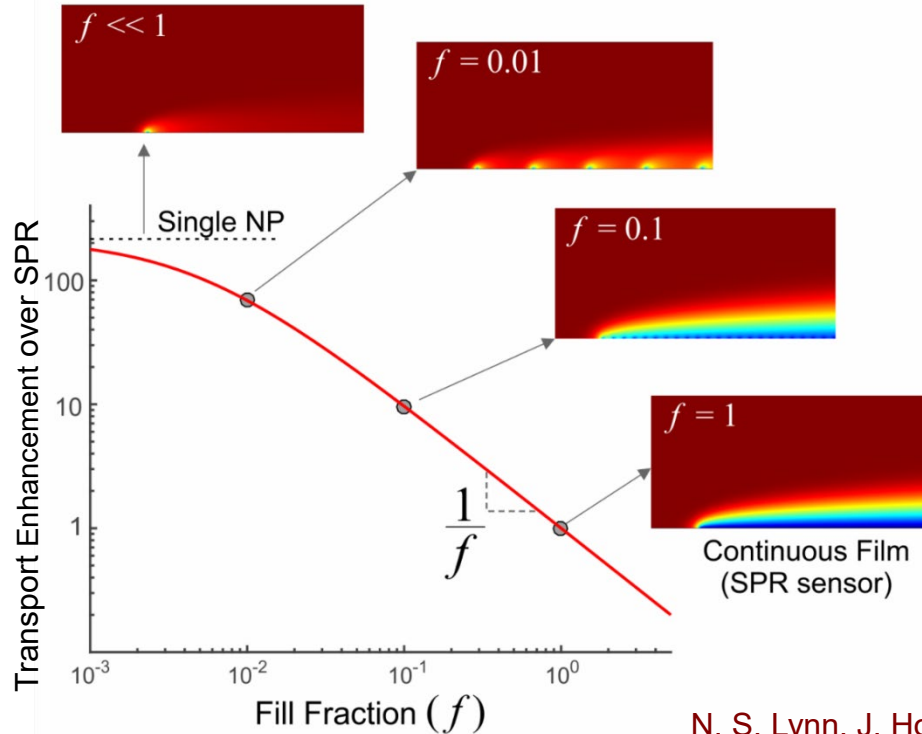
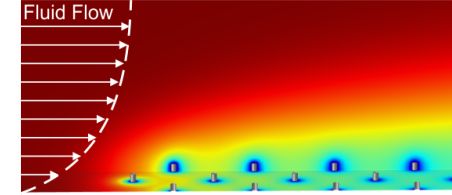
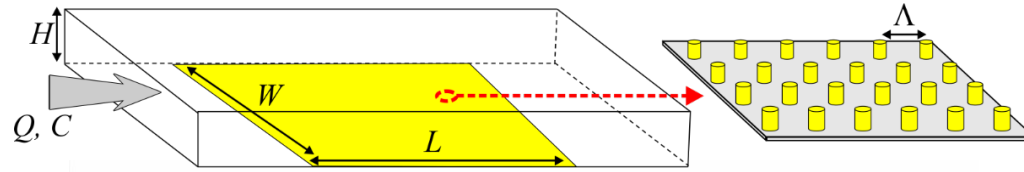
Herringbone structures increase the rate of analyte transport to an active surface of the sensor.



Sensor response improvement by the herringbone micromixer versus Péclet number.

N. S. Lynn, M. Bocková, P. Adam, J. Homola, *Analytical Chemistry*, 87, 5524-5530 (2015).

Analyte transport in plasmonic biosensors



$$f = \frac{\text{Total (active) NP surface area}}{\text{Total surface area of sensing region}}$$

Diffusion-limited transport

$$k_m = \frac{k_m^{NP} - k_m^{SPR}}{\frac{k_m^{NP}}{k_m^{SPR}} f - 2f + 1}$$

N. S. Lynn, J. Homola, *Analytical Chemistry*, 88, 12145-12151 (2016).

Integrating optical and mass transport aspects

Model for the performance of plasmonic biosensor combining the optical performance and mass transport.

Minimum detectable concentration (c_{min}):

Analyte concentration that produces the sensor response corresponding to 3 standard deviations of the sensor output.

$$c_{min} = \frac{3\sigma}{S_{\Gamma}\kappa}$$

σ ... standard deviation of sensor output

S_{Γ} ... sensitivity to surface coverage

κ ... mass transport efficiency

Mass transport efficiency:

$$\frac{1}{\kappa} \approx \left(\frac{1}{k_m} + \frac{1}{k_a\Gamma_0} \right) \frac{1}{T}$$

k_m ... diffusion-limited mass transport coefficient

k_a ... association rate coefficient

Γ_0 ... surface density of receptors

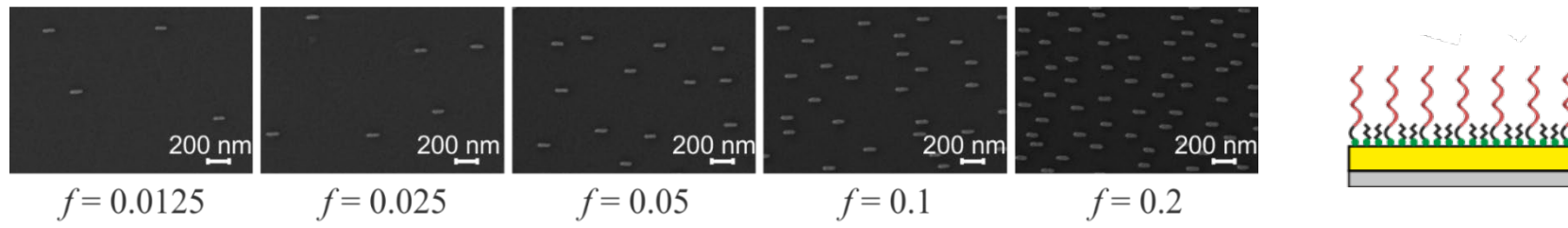
T ... measurement time

N. S. Lynn, J. Homola, *Analytical Chemistry*, 88, 12145-12151 (2016).

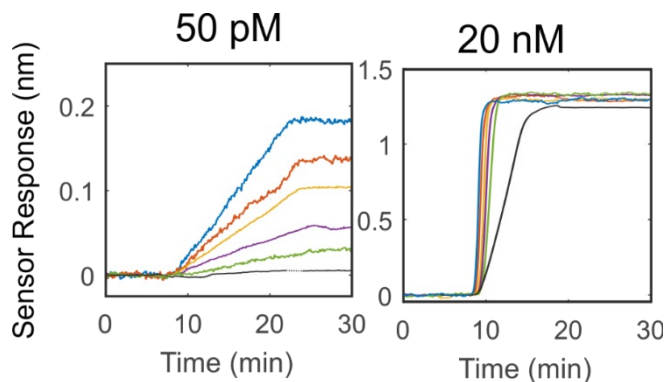
B. Špačková, N.S. Lynn, J. Slabý, H. Šípová, J. Homola, *ACS Photonics*, 5 1019–1025 (2018).

Integrating optical and mass transport aspects

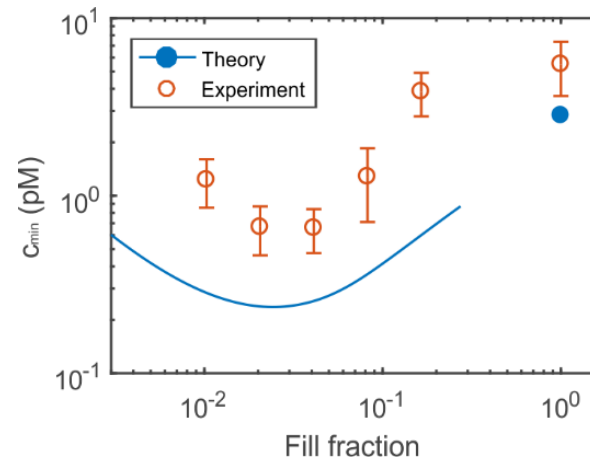
Biosensor based on gold nanorod arrays with different fill fractions.



SEM micrographs of gold nanorod arrays.



Sensor response to two concentrations of analyte for six different fill fractions (left).



Minimum detectable concentration as a function of fill fraction.

C_{min} improvement: **7x**

B. Špačková, N.S. Lynn, et al., *ACS Photonics*, 5 1019–1025 (2018).

Functional coatings

Molecular recognition in plasmonic biosensors

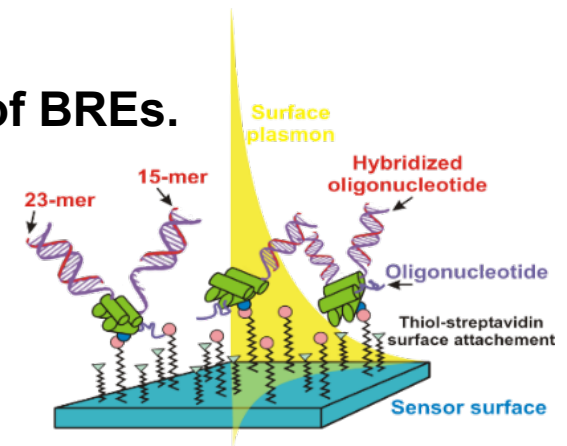
Biorecognition elements (BREs) used in plasmonic biosensors: proteins, antibodies, peptides, aptamers, DNA, RNA, etc.

BREs immobilized on the active surface of a plasmonic structure form a functional coating.

Choice of method for the immobilization of BREs depends on the type of functional molecule, size of target analyte and specifics of application.

Functional coatings – requirements:

1. Preserved structure and functional properties of BREs.
2. Non-fouling background.
3. Favorable orientation of BREs.

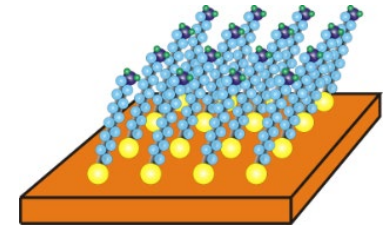


Molecular recognition in plasmonic biosensors

Conventional low-fouling coatings

Poly(ethylene glycol) (PEG) and its derivatives, OEG-alkanethiolate SAMs.

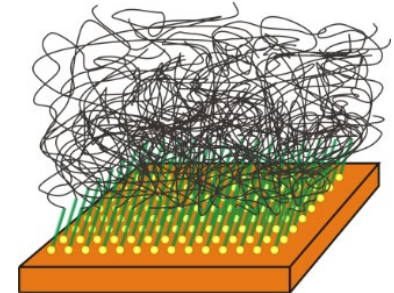
- + Easy to fabricate, various functional groups available.
- Insufficient resistance to fouling from biological media
- 2D nature limits the number of available binding sites



Advanced coatings

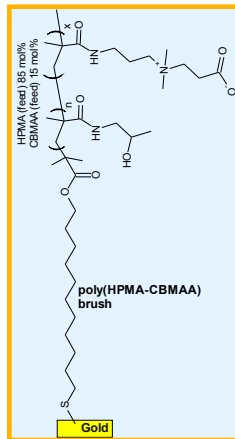
Zwitterionic/non-ionic polymers, hydrogels, polymer brushes.

- + Improved fouling properties.
- + 3D structure with a high number of binding sites.
- Complex to fabricate.

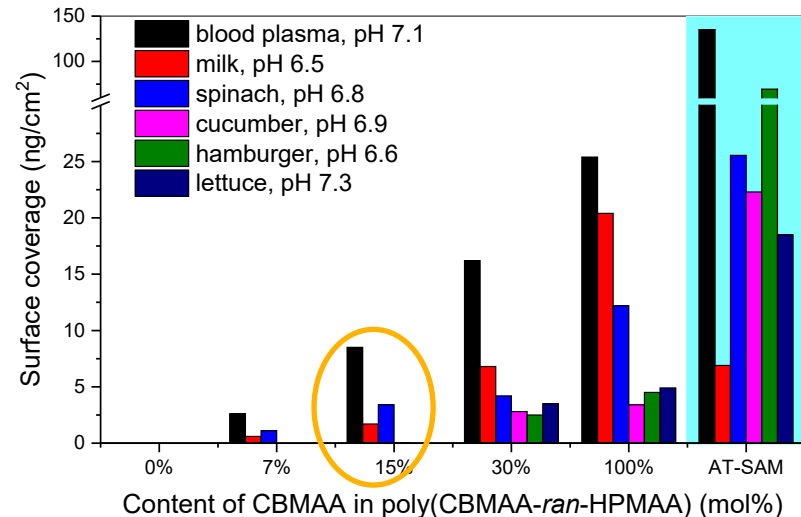


Suppressing non-specific adsorption by advanced coatings

Polymer brush combining functionalization capabilities poly(carboxybetaine methacrylamide) (CBMAA) and fouling resistance of poly(hydroxypropyl methacrylamide) (HPMA).



Poly(CBMAA-ran-HPMAA) brush with carboxylate groups for functionalization.



Non-specific adsorption from complex samples on a functionalized poly(CBMAA-ran-HPMAA) brush as a function of molar content of CBMAA.

H. Vaisocherová-Lísalová, F. Surman, I. Víšová, M. Vala, Tomáš Špringer, et al., *Analytical Chemistry*, 88, 10533–10539 (2016).

NSA improvement: 3-12x

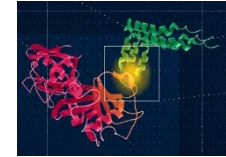
Applications of plasmonic affinity biosensors

Applications of plasmonic affinity biosensors

Plasmonic biosensors are a powerful technology for (i) investigation of biomolecules and their interactions and (ii) detection of molecular targets with unprecedented sensitivity.

Application area #1: Life sciences

Understanding and quantification of complex biological processes (e.g. processes involved in diseases for diagnosis and treatment monitoring).



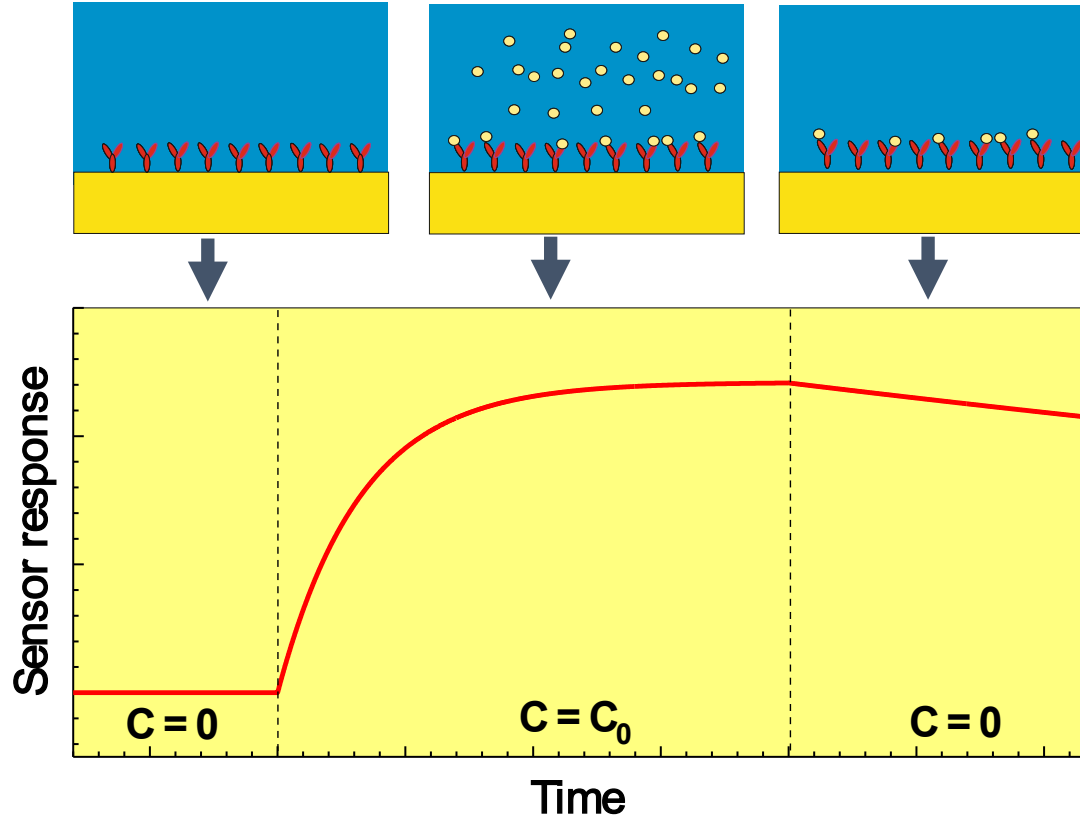
Application area #2: Bioanalytics

Rapid and sensitive detection of biological and chemical species related to:

- healthcare (disease/health biomarkers),
- environmental monitoring (contaminants),
- food safety (pathogens and toxins),
- security (bio/chemical warfare agents).

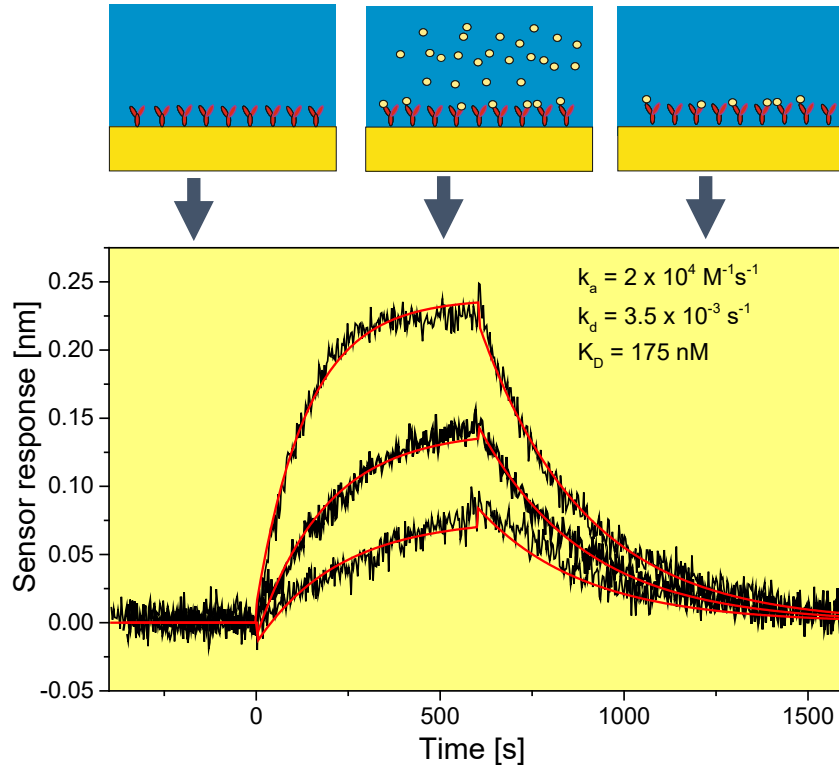


Applications: biomolecular interaction analysis



Sensorgram with a typical sensor response to molecular interactions at the sensor surface.

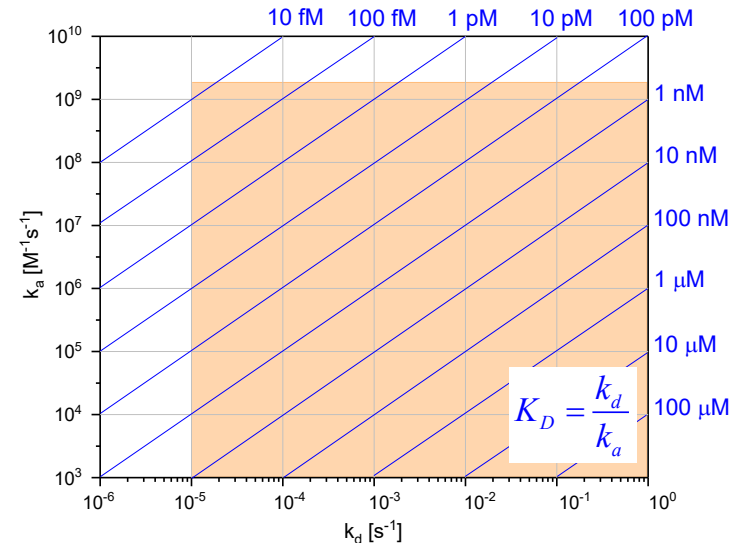
Applications: biomolecular interaction analysis



Typical molecular interaction sensorgram for three different concentrations of free analyte.

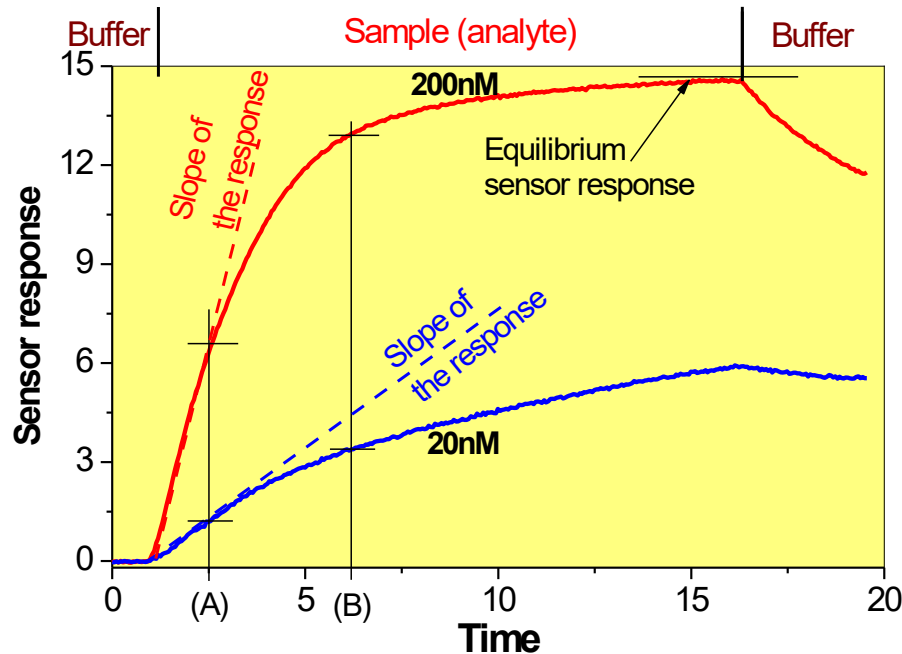
Kinetic equation:

$$\frac{\partial B}{\partial t} = k_a C(R_T - B) - k_d B$$



Space of kinetic rate constants ($k_a - k_d$) covered by plasmonic biosensors.

Applications: detection of biological analytes

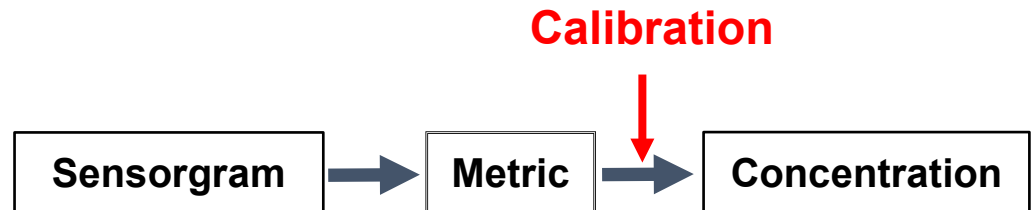


Sensorgram and major sensor metrics.

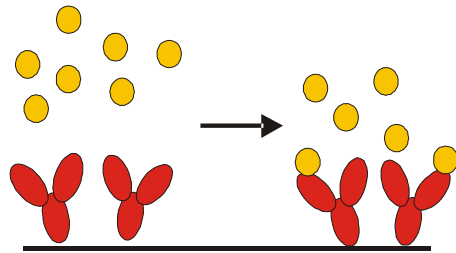
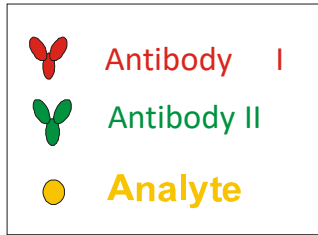
Major metrics:

1. Equilibrium response.
2. Response at a fixed time.
3. Response rate.

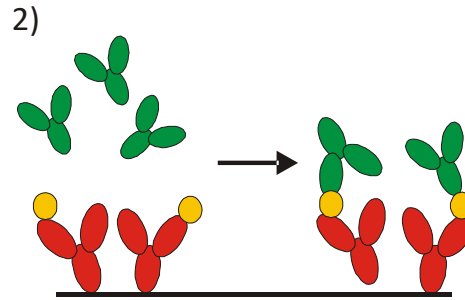
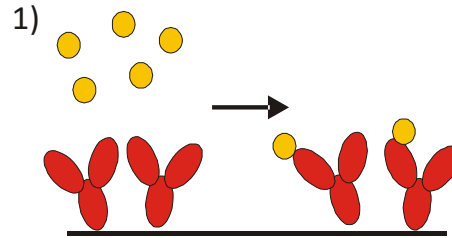
Sensor output processing:



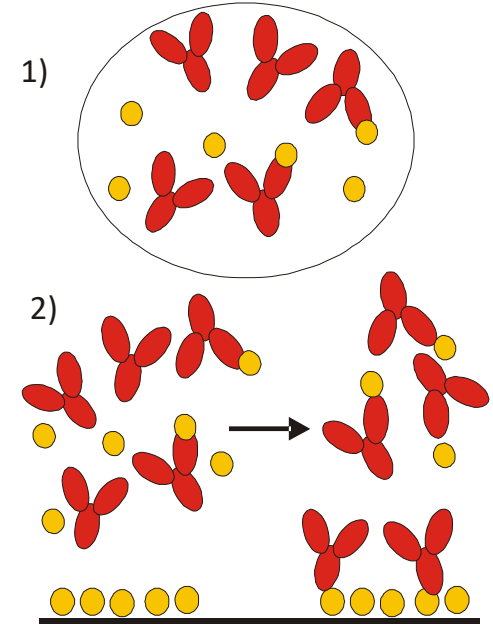
Main detection formats used in conjunction with plasmonic biosensors



Direct detection

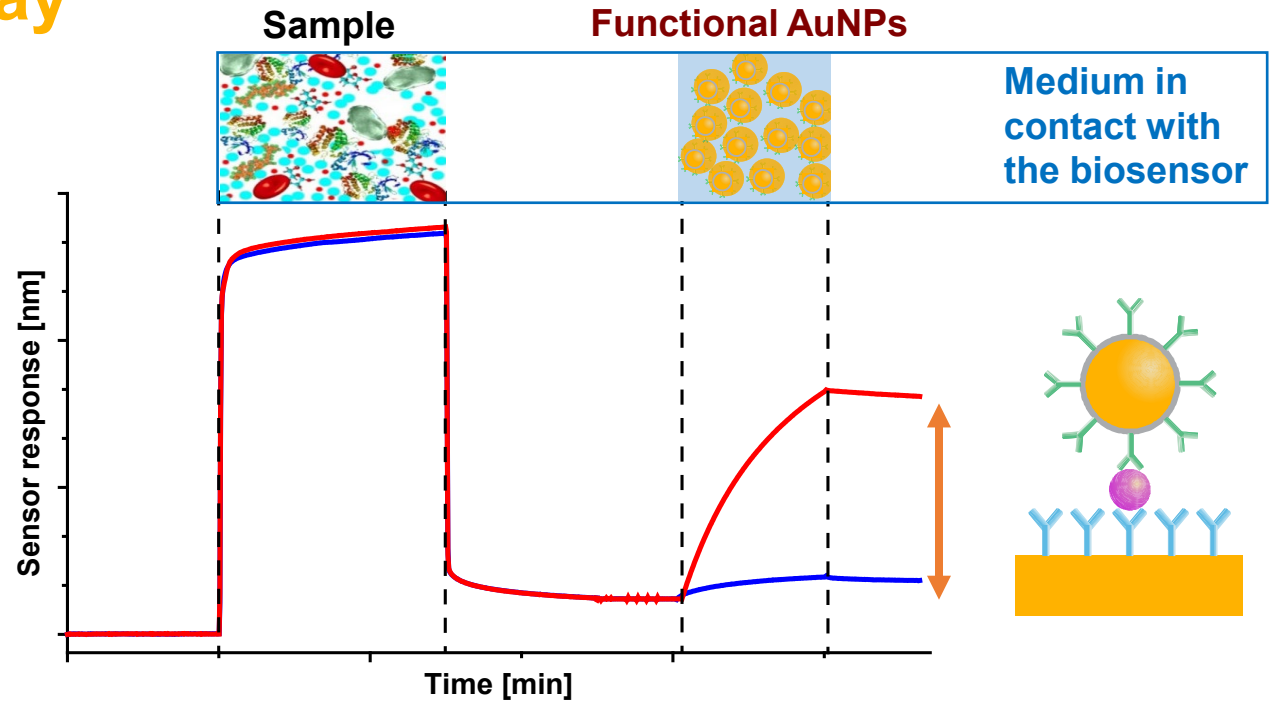


Sandwich assay



Binding inhibition assay

Sandwich assay



Sandwich assay

Specific and non-specific sensor response enhanced by functional AuNPs.

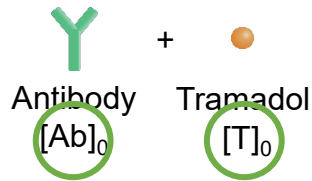
- Improves sensitivity.
- Reduces interferences from complex sample matrix.

T. Špringer, X. Chadtová Song, M. L. Ermini, J. Lamačová, J. Homola, *Analytical & Bioanalytical Chem.*, 409, 4087 (2017).
M. L. Ermini, X. Chadtová Song, T. Špringer, J. Homola, *Frontiers in Chemistry* (2019).

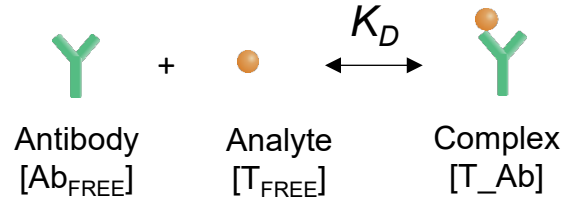
Binding inhibition assay: theory

Reaction of antibody and analyte (tramadol) in a solution.

Initial state:



Equilibrium state:



SPR sensor response $\sim [Ab_{FREE}]$

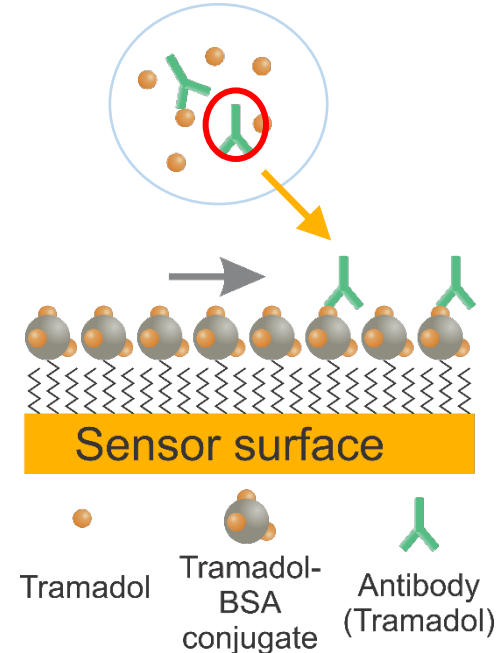
In equilibrium state:

Equilibrium constant:

$$K_D = \frac{[Ab_{FREE}][T]}{[T_{Ab}]}$$

Concentration of unreacted antibody:

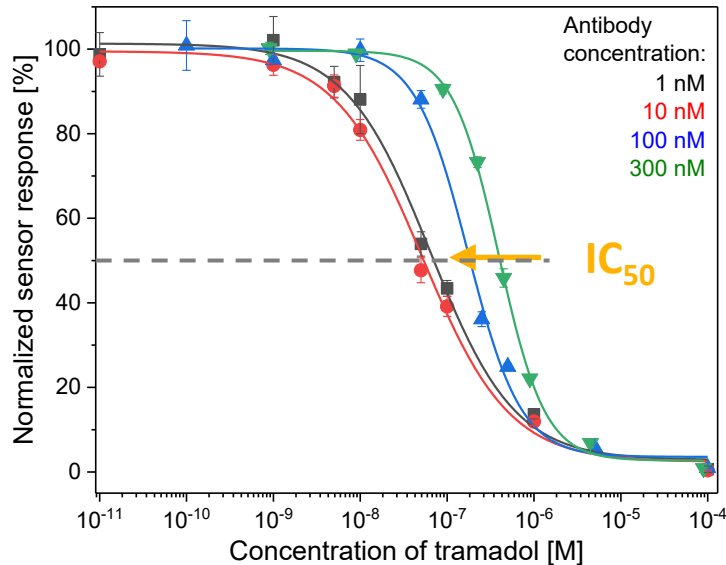
$$[Ab_{FREE}] = \frac{[Ab]_0 - [T]_0 - K_D + \sqrt{([T]_0 + K_D - [Ab]_0)^2 + 4K_D[Ab]_0}}{2}$$



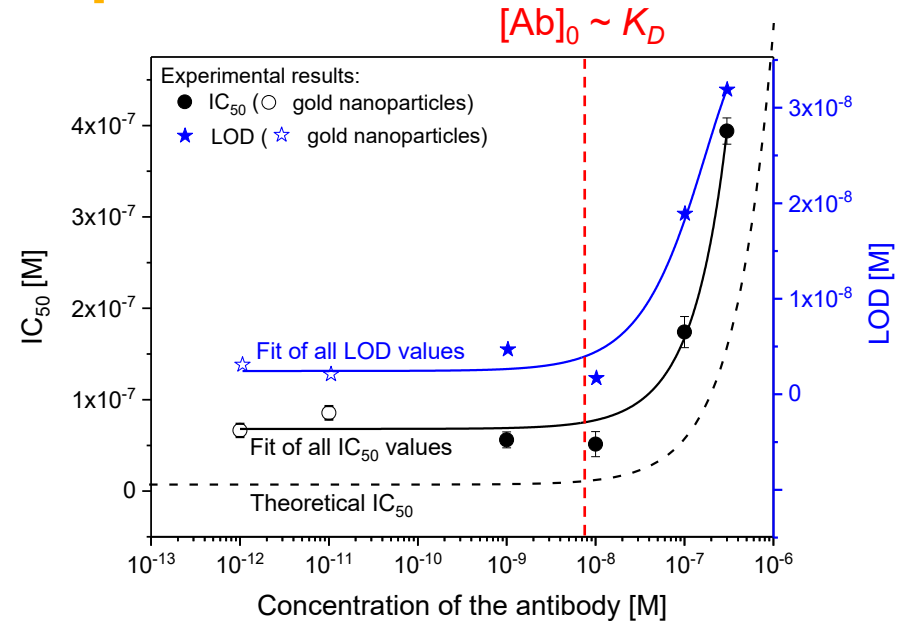
Only 3 initial parameters

E. Hemmerová, et. al., *Sensors & Actuators B: Chemical* 444, 138321 (2025).

Binding inhibition assay: experiment



Experimentally determined calibration curves for different antibody concentrations.



Dependence of IC_{50} and limit of detection (LOD) on the antibody concentration.

Binding inhibition assay

- Decrease of antibody concentration shifts IC_{50} toward lower tramadol levels; this trend stops at $[Ab]_0 \sim K_D$ of tramadol-antibody interaction
- LOD values follow the same trend. The use of AuNPs does not change the trend.

Plasmonic biosensors for bioanalytics

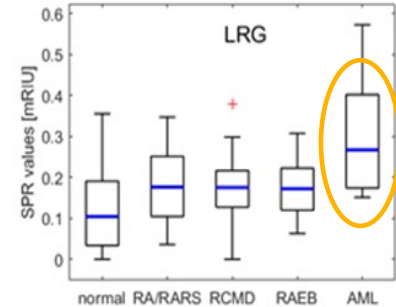
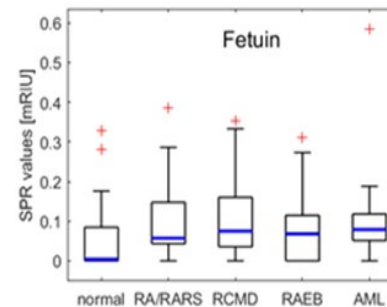
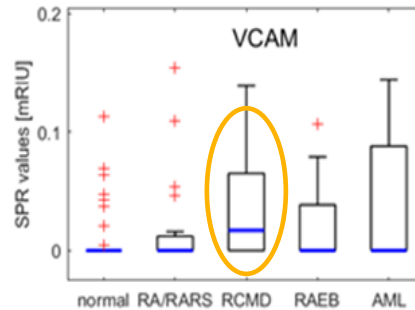
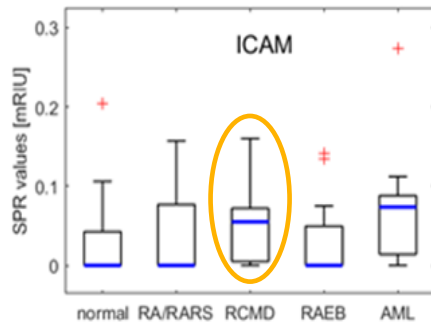
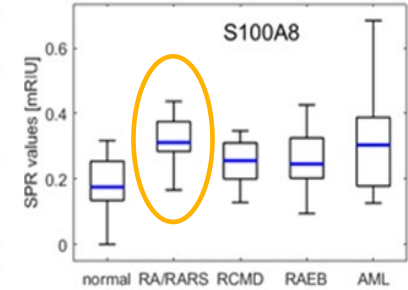
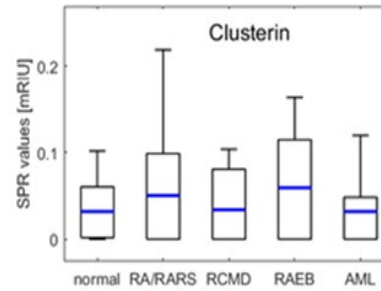
Detection of protein interactions

Clinical study

79 blood plasma samples from MDS subgroups (RA/RARS, RCMD, RAEB), AML patients, and healthy controls.



Sensor responses for plasma samples of MDS subgroups, AML, and healthy controls.



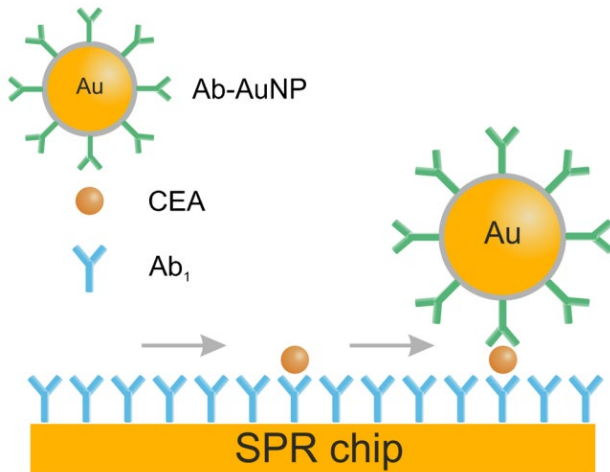
- Large differences among MDS subgroups, AML and healthy controls.
- Prospective diagnostic tool for disease progression monitoring.

L. Chrastinova, et al, *Scientific Reports* 9, 12647 (2019).

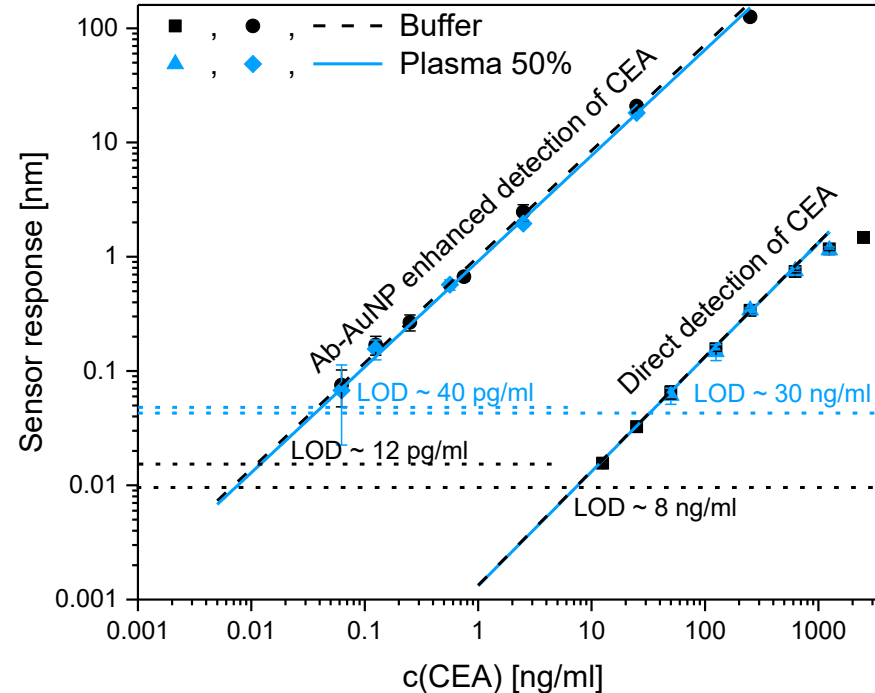
Detection of protein biomarkers

CEA (carcinoembryonic antigen) is a prospective biomarker of gastrointestinal cancer.

Detection format:



LOD in buffer: 12 pg/ml (60 fM)
LOD in plasma: 40 pg/ml (200 fM)

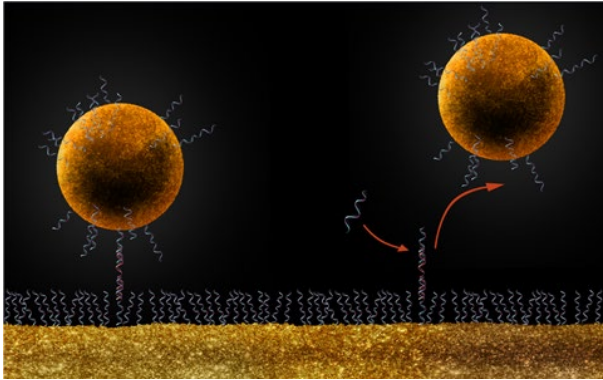


Calibration curves for the detection of CEA in buffer and 50% blood plasma.

T. Špringer, J. Homola, *Analytical and Bioanalytical Chemistry*, 404, 2869-2875 (2012).

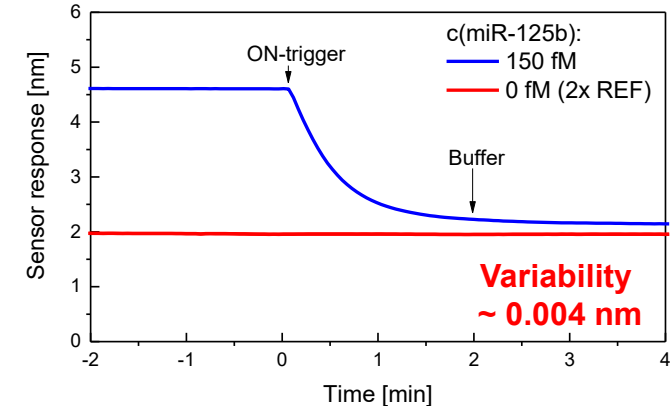
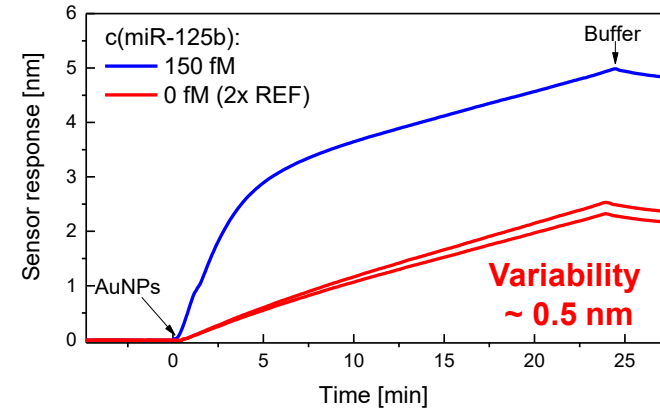
Detection of microRNA biomarkers: NPR assay

Detection of prospective MDS biomarkers - miRNA-16, miRNA-125b.



Nanoparticle release (NPR) assay.

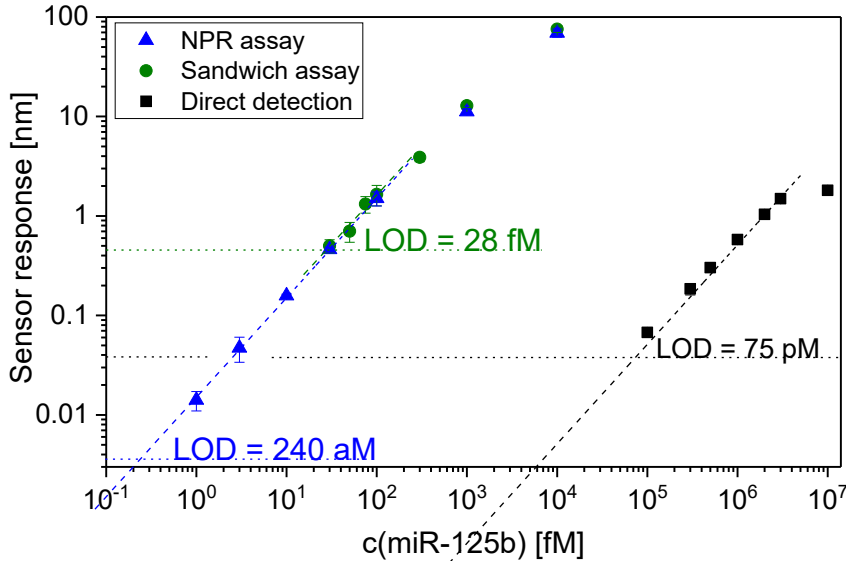
- Performance of sandwich assay is limited by the variability of sensor response (even to blank sample).
- NPR assay reduces the variability by ~2 orders of magnitude.



Detection of miRNA-125b using sandwich and NPR assay: variability of output.

T. Špringer, Z. Krejčík, J. Homola, *Biosensors and Bioelectronics*, 194, 113613 (2021).

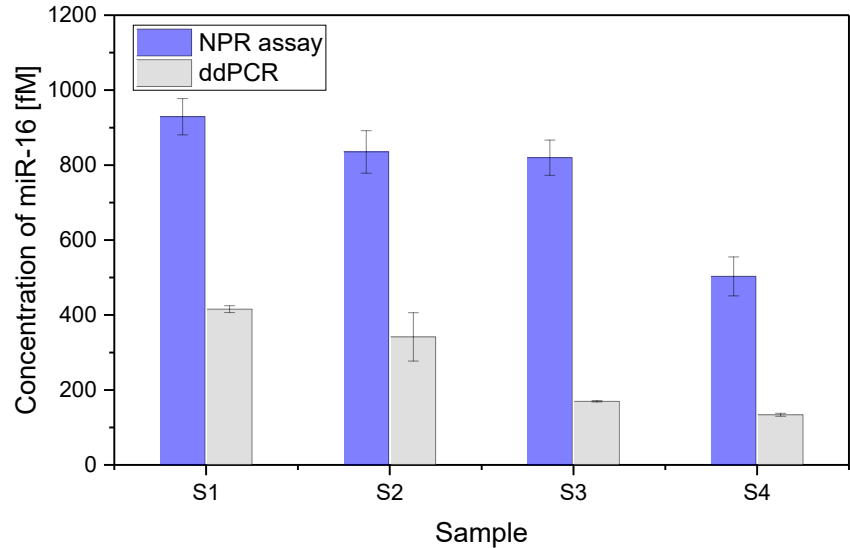
Detection of microRNA biomarkers: NPR assay



Calibration curves for the detection of miR-125b in buffer.

Performance achieved

- LOD reduced by ~100 compared to sandwich assay.
- LOD = 350 aM in blood plasma.



Levels of miR-16 in MDS patients' blood plasma measured with the NPR assay and ddPCR.

Patients' samples analyzed

- Levels of miR-16 in plasma determined (500-900 fM).
- Results compared with ddPCR.

T. Špringer, Z. Krejčík, J. Homola, *Biosensors and Bioelectronics*, 194, 113613 (2021).

Analytical applications of plasmonic biosensors

Small organic molecules

Environmental pollutants

bisphenol A, atrazine, microcystine

Sensors Actuat B 177 (2010)

Anal Bioanal Chem 1618 (2007)



Veterinary drugs

enrofloxacin, chloramphenicol

Biosens Bioel 1231 (2010)

Foodborne toxins

tetrodotoxin, botulinum toxin

Int J Food Microbiol p61 (2001)

J AOAC Int 596 (2011)

10 – 10³ pg/mL

milk, honey, drinking and waste water

Nucleic acids

Gene mutation studies

antisense ONs, single nucl. polymorphism in TP53

NAR 42 (2014)

Anal Bioanal Chem 2343 (2011)



Organ damage, MDS

micro RNA

Biosens Bioel 70 (2015)

Anal Chem 10110 (2010)

Enzymes activity

RAYT, RNaseH

Anal Bioanal Chem 407 (2015)

Biosens Bioel 1605 (2010)

10 aM – 100 fM

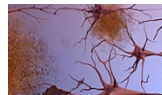
blood plasma, tissue sample, cell lysate

Protein biomarkers

Alzheimer disease

amyloid β , protein Tau

Curr Alzheimer Res 10 (2013)



Cancers

CEA, ALCAM, hCG

Anal Bioanal Chem 2869 (2012)

Biosens Bioel 1656 (2010)

Anal Bioanal Chem 2869 (2012)

Myelodysplastic syndromes

VEGFR

Anal Bioanal Chem 381 (2012)

Immune system

hIFN γ , IL-23

Proteins 82 (2014)

Sens Act B 174 (2012)

10 – 10⁴ pg/mL

blood plasma, cerebrospinal fluid

Pathogenic bacteria

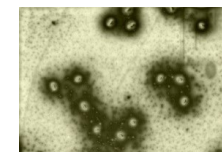
Foodborne pathogens

***Escherichia coli*,
Salmonella enterica,
Listeria monocytogenes,
*Campylobacter jejuni***

Biosens Bioel, 80 (2016)

Sensors Actuat B 59 (2009)

Biosens Bioel 752 (2006)



10 – 10³ cfu/mL

milk, orange juice, meat, cucumber

For more details: <https://www.ufe.cz/en/research/optical-biosensors/>

Conclusions

- Advances in optical platforms, microfluidic systems, functional coatings and detection methodologies have **improved performance and expanded capabilities** of plasmonic biosensors.
- Although **non-specific interactions remain the main challenge** for applications in complex biological media, the number of applications of plasmonic biosensors in **medical diagnosis** has **been growing**.
- Plasmonic biosensors for the **detection of protein and miRNA** biomarkers achieving LODs as low as **$10^1 - 10^2$ aM (miRNA) and $10^1 - 10^2$ fM (proteins)** demonstrated.

Acknowledgement



Collaborators:

- Institute of Hematology and Blood Transfusion, Prague
- Institute of Macromolecular Chemistry of the CAS, Prague

Sponsors:

- Czech Science Foundation
- Czech Ministry of Health
- European Commission

Thank you!